Miniaturization of a micro-optics array for highly sensitive and parallel detection on an injection moulded lab-on-a-chip

Hung, Tran Quang; Sun, Yi; Poulsen, Carl Esben; Than Linh, Quyen; Chin, Wai Hoe; Bang, Dang Duong; Wolff, Anders

Published in:
Lab on a Chip

Link to article, DOI:
10.1039/c5lc00176e

Publication date:
2015

Document Version
Publisher's PDF, also known as Version of record

Lab on a Chip

PAPER

View Article Online
View Journal

Cite this: DOI: 10.1039/c5lc00176e

Miniaturization of a micro-optics array for highly sensitive and parallel detection on an injection moulded lab-on-a-chip†‡§

Tran Quang Hung,[ab] Yi Sun,[a] Carl Esben Poulsen,[a] Than Linh-Quyen,[b] Wai Hoe Chin,[b] Dang Duong Bang[b] and Anders Wolff*[a]

Received 12th February 2015,
Accepted 9th April 2015

DOI: 10.1039/c5lc00176e

www.rsc.org/loc

A miniaturised array of supercritical angle fluorescence (SAF) micro-optics embedded in a microfluidic chamber was fabricated by injection moulding. The fabricated chip could enhance the fluorescence signal around 46 times compared to a conventional microscope. Collection of the fluorescence signal from the SAF array is almost independent of the numerical aperture, and the limit of detection was improved 36-fold using a simple and inexpensive optical detection system.

Introduction

Although many advanced technologies such as Raman spectroscopy[1] and magnetic based platforms[2] have been developed for highly sensitive detection of biomolecules, fluorescence-based sensing technology is still the most widely used technique and has been so for several decades.[3] Many research studies are therefore devoted to improve the sensitivity of fluorescence detection, *e.g.* by using a thin layer of metallic nanoparticles on a microscope slide to enhance light–plasmon coupling[4–6] or a super-resolved fluorescence microscope, which transcend Abbe's diffraction limit of half of the utilized wavelength ($\lambda/2$).[7–11] Even though such methods can achieve unprecedented resolution and have a detection limit down to a single photon, they require very expensive optical equipment and have a very limited field of view. Such methods are therefore normally limited to central research laboratories.

Alternatively, another highly sensitive detection method based on supercritical angle fluorescence (SAF) microscopy was described by J. Enderlein *et al.*[12] SAF is based on the principle that fluorescent molecules near the interface of two media with different refractive indices radiate highly asymmetrically. The majority of the light is emitted into the higher refractive index medium, mainly around the supercritical angle (θ_c). This main portion of the fluorescent light is lost in the conventional system, but in the so-called SAF microscopy,[13–19] a parabolic lens system has been developed as a microscope objective to collimate the light emitted into the higher refractive medium. C. M. Winterflood *et al.* reported that by collecting the fluorescence signals above and below θ_c, the SAF microscopy system became extremely sensitive to the z-position.[20] It was possible to discriminate surface-bound targets (within 100 nm from the surface) from the targets in the sample solution. This eliminates fluorescence "noise" from the liquid and enables a real-time study of binding kinetics at the interface. However, a conventional SAF setup measures only one detection point, which limits its application in array-based sensing. To overcome this limitation, D. Hill *et al.* introduced a polymer biochip with an array of integrated 3 × 3 parabolic SAF structures with a diameter of 3 mm and a pitch of 4.5 mm.[21] This chip has the advantages of SAF microscopy (excellent sensitivity and good discrimination between molecules on the surface and in bulk solution) coupled with the multiplex detection capability of micro-array technology. Nevertheless, such a large-size array has several disadvantages such as having a limited number of detection points and requiring a large volume of sample. Miniaturization of SAF structures will provide more dense arrays to increase the multiplex detection capability. However, fabrication of high-quality micro-lens with a parabolic shape is extraordinarily difficult and requires sophisticated know-how and clean-room fabrication expertise.[22] To our knowledge, there has been no report on minimization of SAF

[a] *DTU Nanotech, Department of Micro- and Nanotechnology, Technical University of Denmark, Ørsteds Plads, DK-2800 Kgs. Lyngby, Denmark. E-mail: anders.wolff@nanotech.dtu.dk; Fax: +45 45 88 77 62; Tel: +45 45 25 63 05*

[b] *Laboratory of Applied Micro and Nanotechnology (LAMINATE) National Food Institute, Technical University of Denmark (DTU-Food), Denmark*

† The authors declare no competing financial interests.

‡ Anders Wolff, Tran Quang Hung and Dang Duong Bang designed the research plan. Tran Quang Hung, Yi Sun, Wai Hoe Chin, and Than Linh-Quyen performed the experiments; Carl Esben Poulsen and Tran Quang Hung performed the calculations. The paper was written by Tran and was revised by all the co-authors.

§ Electronic supplementary information (ESI) available. See DOI: 10.1039/c5lc00176e

array and this is still a big technological challenge. Here, we addressed this challenge by introducing a truncated cone-shaped SAF structure. The cone-shaped structure can collect light at a large collection angle, and it can easily be fabricated by combining micro-milling and injection moulding techniques.

In this paper, we advance our research into the SAF array[2,3] by fabricating a disposable chip with a miniaturised SAF array integrated into a microfluidic chamber for collection of fluorescence signal. The work involves the calculation of the proportion of light emitted into different polymer substrates and the simple fabrication techniques for minimization of the SAF array with low surface roughness. Furthermore, we constructed a low cost optical read-out setup using off-the-shelf components to measure the signal from the SAF array. Finally the low detection limit of the system was determined.

The platform provides a much more sensitive and specific biophysical tool for applications that demand parallel analysis of molecular interactions in sub-nanolitre volumes. It can be widely used in molecular biological and genomic research, *e.g.* gene expression and point mutation/single-nucleotide polymorphism (SNP) analysis.

Materials and methods

Injection moulding of the chips

The injection moulding insert was milled in hard aluminium (alloy 2017, MetalCentret, Denmark) using a computer-controlled micro-milling system (Folken Ind., Glendale, California, USA) followed by polishing (metal polish, Autosol, USA). Arrays of 32 truncated cone-shaped holes were milled using a 60° milling tip DIXI 7006 (DIXI, Le Locle, Switzerland) as a master for injection moulding of the SAF arrays.

The chips had the dimensions of a microscope slide (76 mm × 25 mm × 1 mm) and were moulded in-house in polystyrene (PS) 158 K (BASF SE, Germany) using a Victory 80/45 Tech injection moulding system (Engel, PA, USA). The chip has eight parallel chambers located at the centre of the chip with a pitch of 9 mm. Each chamber had a volume of 10 μL and contained a miniaturized SAF array of 32 truncated cone-shaped structures. The dimensions of the polymer chip, the microfluidic chamber and the SAF structure are illustrated in Fig. 1. Microfluidic channels were connected with a multichannel pipetting system through 0.8 mm diameter holes at inlets and outlets. A 254 μm thick film of cyclic olefin copolymer (COC) was bonded on the chip using an ultrasonic welder (USP 4700, Techsonic, Herstad + Piber, Denmark) with a trigger force of 750 N, an energy of 70 W s, and a hold time of 0.35 s.

Measurement of the surface roughness

Surface roughness of the SAF structures will give light scattering effects, especially at the sidewall of the SAF structures where the fluorescent light is collected using total internal reflection (TIR, see results in Fig. 4e and f). To characterize the roughness of the sidewall surface, we engineered a holder with a slope angle of 60 degrees and then mounted a piece of the injection moulded SAF structure on this surface to level the sidewall relative to the instrument. The roughness of the SAF structures was characterized using a PLu Neox 3D optical profiler (Sensofar, USA) with a vertical resolution of less than 2 nm.

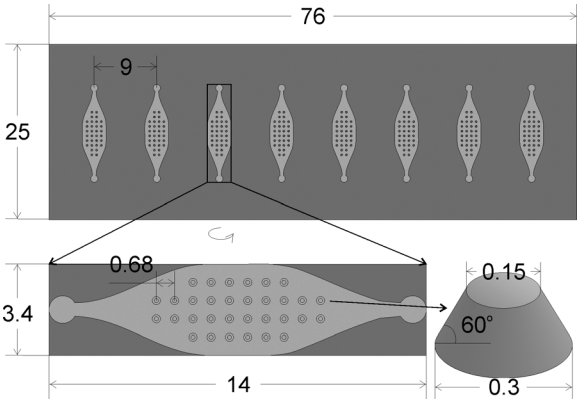

Fig. 1 Schematics illustrating dimensions of a polymer chip, a microfluidic chamber and a SAF structure (all dimensions are in mm). The pitch between the SAF structures is 0.68 mm to avoid interference of fluorescent light from nearby SAF structures.

Detection system

We developed a simple and inexpensive optical setup for detection of Cy3 fluorescence signal from the SAF array as illustrated in Fig. 2. The optical setup is composed of off-the-shelf components: a green solid state laser (532 nm, 200 mW) (DX, Hong Kong, China) was expanded 4 times using a beam expander with two achromatic lenses: f_1 = 19 mm, Ø = 0.5″, and f_2 = 75 mm, Ø = 1″ (Thorlabs, New Jersey, USA). The central part of the expanded beam, which had an intensity variation of less than 0.3%, was used to illuminate the entire SAF array. The filter cube for Cy3 fluorescence included a 45° green dichroic mirror with a 532 nm ± 8 nm/650 nm ± 8 nm

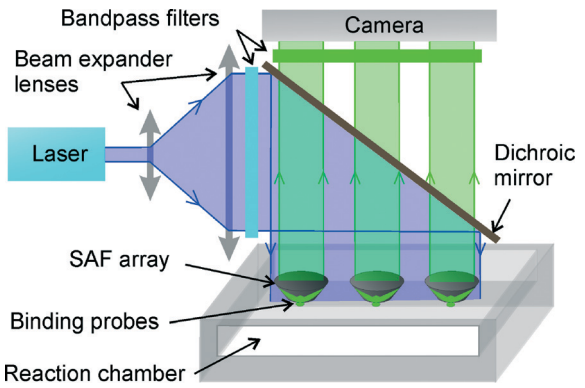

Fig. 2 Working principle of the optical setup to measure fluorescence signal from a SAF array.

reflection/transmission band and band-pass filters of 532 ± 10 nm (Kunming Yulong, China) and 620 ± 26 nm (Thorlabs, New Jersey, USA) for excitation and emission, respectively. The emission light from the SAF array was recorded using a Prosilica camera (EC1380, Allied Vision, USA) with a numerical aperture (NA) of 0.12.

Deposition and immobilization of the probes

A DNA oligonucleotide probe with a poly(T)10–poly(C)10 binding sequence was used for testing the system. The binding sequence enabled direct immobilization of the probe to the plastic substrates by using a simple UV cross-linking technique described previously.[24] The probe was labelled with Cy3 at the 5′ end for visualization. The probe was diluted in a 150 mM sodium phosphate buffer (pH = 8.5) containing 0.004% Triton X to final concentrations from 3.15 pM to 31.5 μM. Spotting was performed using a noncontact array nano-plotter 2.1 (GeSim, Dresden, Germany) fitted with a picoliter pin (Pico-Tip J, GeSim, Dresden, Germany). 100 pL drops of the DNA probe were spotted onto the top of each SAF structure, resulting in a spot size of approximately 70 μm. The chips were incubated at 37 °C for 10 min and then exposed to UV irradiation at 254 nm with an energy density of 0.3 J cm^{-2} using Stratalinker 2400 (Stratagene, CA, USA). Hereafter, the chips were washed with 0.1× standard saline sodium citrate (SSC) solution containing 0.1% (w/v) sodium dodecyl sulphate (SDS) (Promega, WI, USA), and rinsed with deionized water followed by drying using nitrogen gas.

Results and discussion

Selection of polymers and design of the SAF structure

In many applications, the fluorophores in a DNA array are detected on a dry substrate. However, for real-time analysis in a microfluidic system the DNA array will be covered with a buffer solution. To select a suitable substrate for fabrication of the disposable chips, we calculated the proportion of the light emitted into the chip part as a function of its refractive index for two interfaces: air/substrate and water/substrate. In the calculation, we considered that the fluorescent molecule (dipole) emits light into the lower refractive index environment n_1 by two terms, reflection and scattering, whereas the light emitted into the higher refractive environment n_2 only consists of a transmission term. The intensity of the light emitted into the substrate as a function of the refractive index was calculated analytically as given in Fig. 3 [see S1† for details].

The results in Fig. 3 reveal that the fluorophores on the interface of the air/substrate emits a higher portion of the fluorescence intensity into the substrate than that on the water/substrate interface. Moreover, the higher the refractive index of the substrate, the greater the portion of the fluorescent light is emitted into it. As seen in Fig. 3, PS has a high light collection proportion and, furthermore, it is the most commonly used thermoplastic for laboratory cultureware and

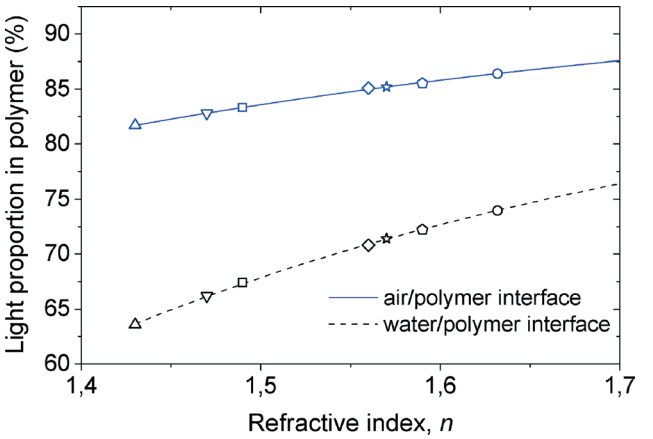

Fig. 3 The proportion of the fluorescence intensity emitted from a fluorophore sitting on the interface into the polymers (chip part) as a function of the refractive indices of air/polymers (blue curve) and water/polymers (black curve), respectively. The symbols represent glass and polymers with different refractive indices: △ PDMS (n = 1.43); ▽ Pyrex glass (n = 1.47); □ PMMA and PP (n = 1.49); ◇ COC (n = 1.56); ☆ PET and PC (n = 1.58); ⬠ PS (n = 1.59); and ○ PE (n = 1.63).

utensils.[25] Additionally, good transparency and low cost make PS an excellent polymer for replication of the SAF structures.

To design the chip, we calculated the distribution of the fluorescence intensity emitted into the PS substrate for fluorophores on air/PS and water/PS interfaces. The polar plot and 3D graph of the fluorescence intensity distribution in the two media are calculated from eqn (1) and (2) in S1† and given in Fig. 4. The calculations reveal that the fluorescence intensities radiated into the PS substrate are 85.56% and 72.1% of the total intensities for air/PS and water/PS interfaces, respectively. A parabolic lens is the best structure to collimate these proportions of fluorescent light. However, it is very difficult to fabricate such a structure on a small scale. In this work, we introduce a truncated cone-shaped SAF structure with high collection efficiency, which is shown schematically in Fig. 4e. Theoretically, this truncated SAF structure can collect light at emission angles of up to 79.2° and 63.2° for air/PS and water/PS interfaces, respectively (the maximum angle for total internal reflection). The fluorescence intensities collected by using these new truncated cone SAF structures are calculated to be about 98% (air/PS) and 78% (water/PS) of the total fluorescence intensities collected by using a perfect parabolic lens. These are excellent collection efficiencies; the truncated SAF structure is therefore suitable for detection of fluorophores on both air/PS and water/PS interfaces.

Characterization of the polymer chips

SEM images of the miniaturized SAF array of 32 structures on the aluminium mould are illustrated in Fig. 5a and b. An image of an injection moulded PS chip with 8 chambers with SAF arrays is given in Fig. 5c.

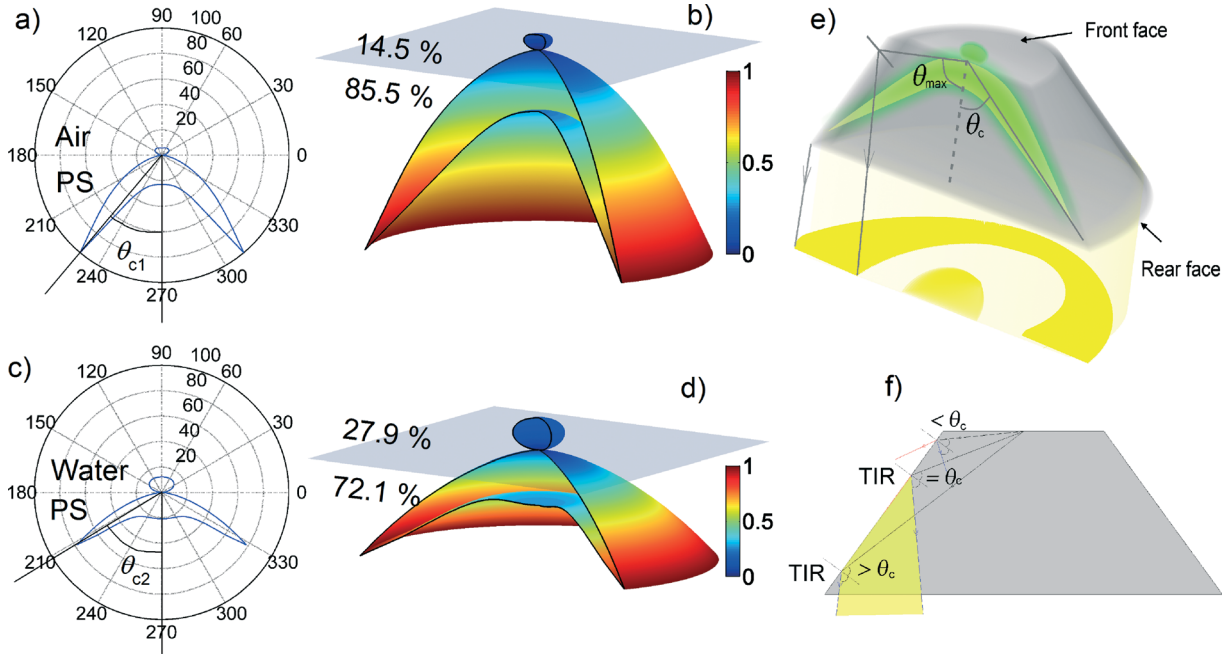

Fig. 4 (a–b and c–d) Theoretical calculations shown as polar plots and 3D surfaces (using eqn (1) and (2) in S1†) of the light intensity of fluorescent molecules distributed on air/PS and on water/PS interfaces. e) Schematic of the truncated-cone SAF structure for high efficiency collection of fluorescence signal. f) Schematic of fluorescent light collection at the sidewall of a SAF structure. At $\theta \geq \theta_c$, there is total internal reflection at the sidewall, and the fluorescent light is collected by the SAF structure. At $\theta < \theta_c$, the light is transmitted and only a small part of it is reflected and collected by the SAF structure.

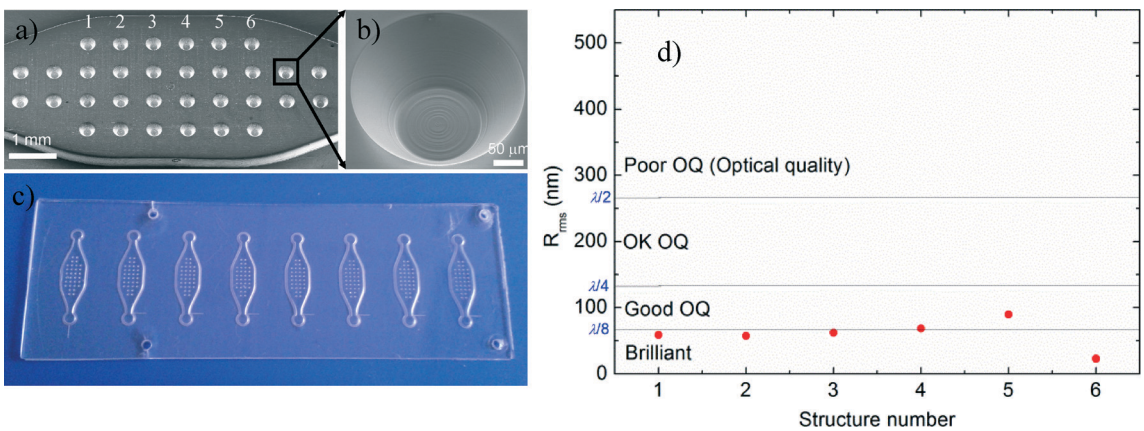

Fig. 5 a) SEM image of an array of 32 SAF structures inside a 10 μL chamber on the mould insert. b) SEM image of one structure. c) Image of a PS chip. d) Roughness of different SAF structures (same number as indicated in a).

The surface roughness of the SAF structures shown in Fig. 5d was measured using an optical profilometer. The sidewall images were analysed by using two parameters with Gaussian filter function: one describing the curvature and another describing the roughness of the structure [see details in S2†]. The vertical resolution of these measurements is smaller than 2 nm. The average roughness values of the two PS SAF arrays replicated from polished and unpolished inserts were determined to be 68 nm ± 4.8 nm and 92 nm ± 15 nm, respectively. Consequently, the polishing reduces the roughness of the SAF structure by about 25% compared to the unpolished structures. The roughness of the polished structures reaches a brilliant optical quality range (~λ/8) with small variance of about 7%.

Signal amplification by the SAF structures

Fig. 6a depicts the fluorescence images of an array captured from the front face and the rear face of the SAF array using a microscope with a 5× objective and a numerical aperture of 0.12. The intensity cross section of a fluorescence spot measured from both the rear and the front faces of a SAF structure is plotted in Fig. 6b as solid and dot lines, respectively. The intensities are determined as grey values of the

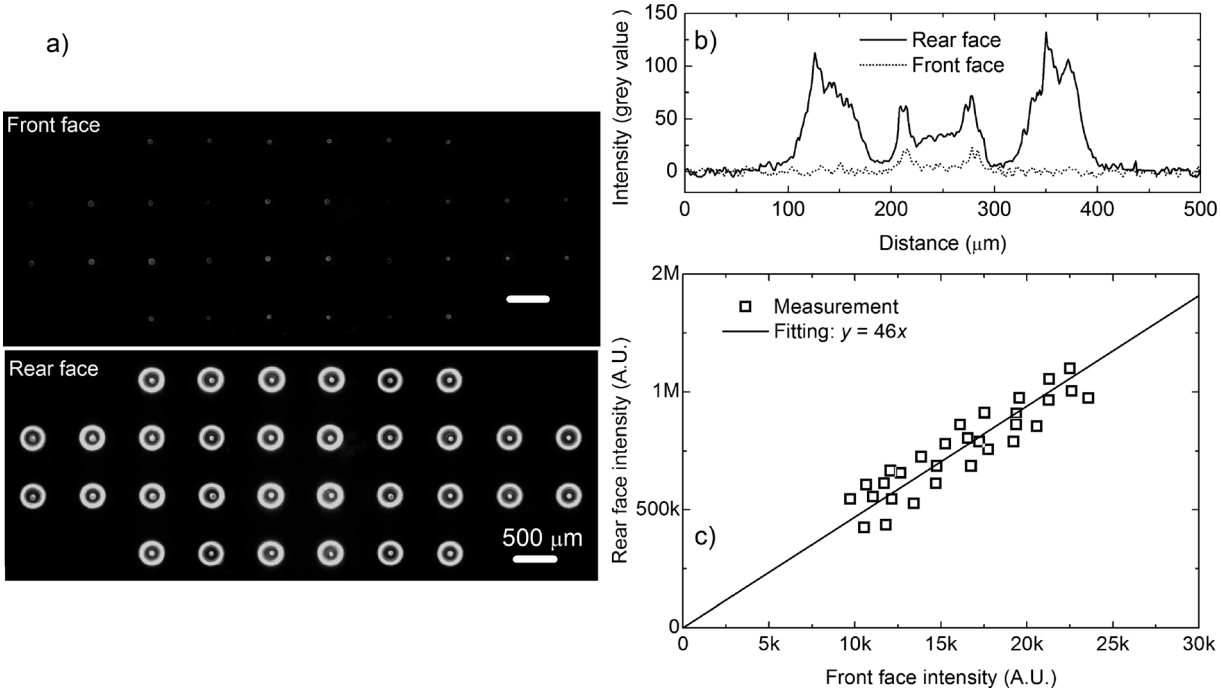

Fig. 6 a) Montage of fluorescence images of the spot array captured from the front face of the SAF structure (top image) and from the rear face of the SAF structure (bottom image). b) The fluorescence intensity plotted in greyscale across one spot measured from the front face (dotted line) and from the rear face (solid line). c) Plot of the fluorescence intensity measured from the rear face of the SAF array *versus* the integrated fluorescence intensity measured from the front face of the SAF array.

fluorescence signal from fluorescence images using ImageJ software.[26] Evident in Fig. 6b, the intensity measured from the rear face (where the SAF structure is used) is much greater than that measured from the front face (corresponding to conventional systems).

For quantification, the integrated fluorescence intensity emitted from the rear face is plotted *versus* the intensity from the front face of the whole SAF array as depicted in Fig. 6c. There is a linear relationship which reveals that the SAF array increases the fluorescence signal around 46-fold.

This high signal amplification achieved using the SAF structure is ascribed to two factors:

(*i*) A greater portion of the fluorescence signal is emitted into the PS substrate than that into air. As indicated in Fig. 4b, the fluorescence intensity in PS is about 5.9 times higher than that in air.

(*ii*) The collection efficiencies in the two environments are different: in the low refractive medium (air, n_1), the collection efficiency is proportional to the numerical aperture (NA) of the optical system ~ NA × sin(θ_1) (where θ_1 is the collection angle of the objective), due to the approximately even distribution of the emission in all directions. In the high refractive medium (PS substrate, n_2), the SAF structures collect the fluorescent light within the angle range from 40.8° to 79.2° due to the total internal reflection at the sidewalls of the SAF structures (Fig. 4e). Our calculations show that about 98% of the total fluorescent light emitted into the PS substrate was collected using the SAF structures, and the light collection efficiency is therefore largely independent of the NA of the objective of the optical system (Fig. 7a).

Thus the signal ratio between the fluorescence signals from the rear face and the front face of the SAF structures is a function of the NA as depicted in Fig. 7b; the measured data and the calculation are plotted as circles and a solid line, respectively. In this figure, the data were collected using microscope objectives of 5×, 0.12, 4.4 mm; 10×, 0.3, 2.2 mm; 20×, 0.46, 1.1 mm; 50×, 0.5, 0.44 mm; and 100×, 0.8, 0.22 mm (magnification, NA and diameter of the field of view, respectively). In the calculation, we considered ratios between the signal collected by the SAF structures within the angle θ_{max} = 79.2° in the PS substrate and the signal collected in the air medium with NA from 0.12 to 1 corresponding to the angle θ_1 varying from 6.9° to 90°. The calculated signal ratios are higher than the measured ones, which may be ascribed to some light scattering from the sidewall of the SAF structures (due to surface roughness) [see S3† for details] and a little transmission loss in the PS. As shown in Fig. 7b, a higher NA objective leads to a lower signal ratio because the collection efficiency on the front face of the SAF structure is increasing with the NA of the optical system. But a higher NA objective either has a smaller field of view as indicated in the square brackets under the measurement data in Fig. 7b or requires a larger lens. In these scenarios, the SAF structures reveal prominent advantages of having both high sensitivity and a large field of view, which are desirable for high sensitive detection of multiple targets in a large area.

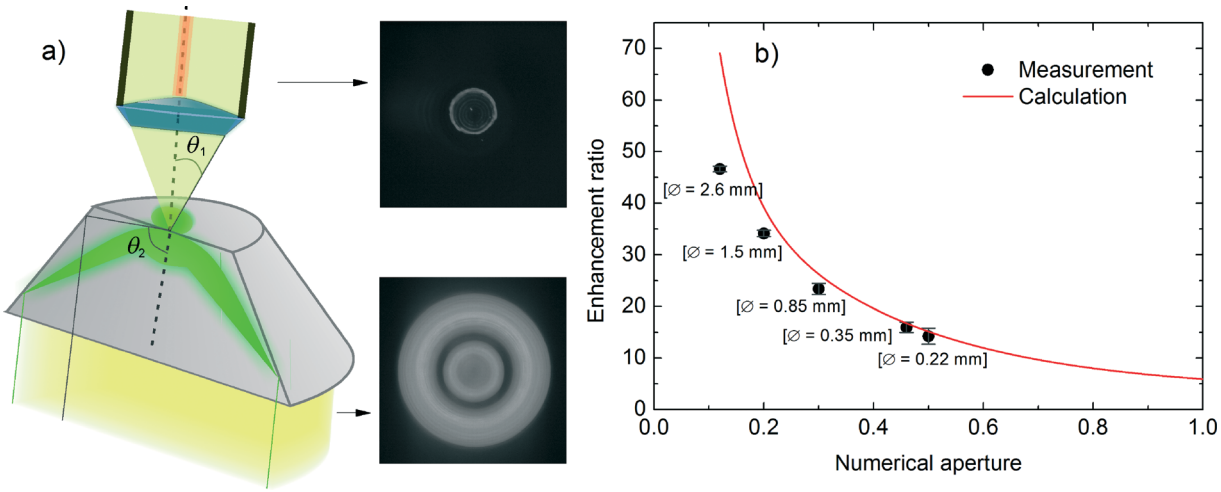

Fig. 7 a) Schematic of signal collection from the front and rear faces of a SAF structure; the two pictures on the right depict the fluorescence images from the two faces. The light collected from the front face is emitted in all directions making the collection efficiency highly dependent on the numerical aperture of the optical device. In contrast, a large portion of the light from the rear face is collected by the SAF structure due to a large collection angle. b) The signal amplification by the SAF structure *vs.* numerical aperture of the microscope objectives. The solid line is the calculation and the circles are measurement points. The numbers under the measurement data represent the diameters of the field of view of the optical system.

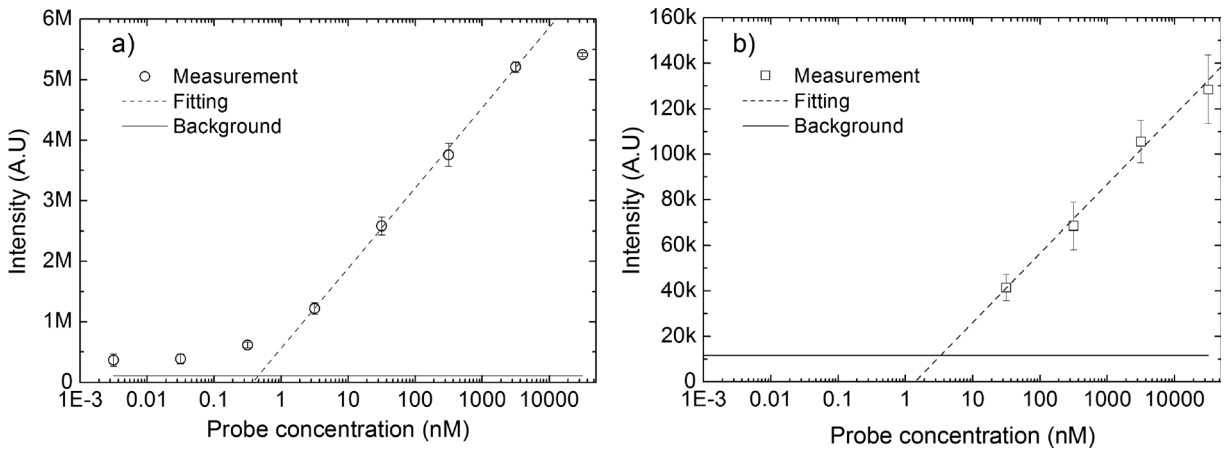

Fig. 8 The intensity of the signal *vs.* probe concentration a) measured from the rear (PS) face (using the SAF structures) b) and measured from the front (air) face using a simple optical setup. These curves correspond to the signal measured by the SAF array and conventional micro-array, respectively.

Limit of detection of the integrated LOC system

To determine the detection limit of the SAF array using a simple and low cost optical system, the fluorescence signal of the Cy3-labelled DNA probe was measured on the SAF array using a 10-fold dilution series with concentrations ranging from 3.15 pM to 31.5 μM. The signal at each concentration was measured from the whole array with a 0.1 nL droplet on each SAF structure (Fig. 8a). The limit of detection (LOD) of the SAF array was calculated using the equation LOD = 3.3 × SD/slope, where SD is the standard deviation of the background signal, and the slope was obtained from linear fitting of the data points. The LOD of the SAF array was determined to be as low as 0.5 nM corresponding to 13 fluorescent molecules per μm^2. The LOD of the signal measured from the front (air) face of the SAF structures using the same optical system is determined to be 18 nM, corresponding to 468 fluorescent molecules per μm^2 as illustrated in Fig. 8b. Thus the use of SAF structures enhances the detection limit of the system by 36-fold. This factor is smaller than the signal increase by the SAF array as discussed in Fig. 6 due to scattering from the sidewall surface of the SAF structure contributing to the background signal.

Conclusions

In this paper we have presented a novel disposable chip with a miniaturised SAF array integrated into a microfluidic chamber for highly sensitive detection of fluorescent molecules.

The micro-optical SAF structures were realized by combining micro-milling of a mould insert and injection moulding. The light intensity distributed in the two media has been calculated for different refractive indices, and based on these data, PS was selected as a suitable material for replicating the SAF array. The presented SAF array reveals great advantages for multiplexed detection. It offers high sensitivity in combination with a large field of view, since light collection efficiency is largely independent of the numerical aperture of the optical system. It also provides high array density, which increases the multiplexing capability for detection of biological targets. Moreover, the detection sensitivity is very high. Fluorophore concentrations as low as 13 molecules per μm^2 could be detected using a cost effective optical readout system. In further development, a lower detection limit could be achieved by reducing the background signal and by using higher wavelength fluorophores such as Cy5, which could minimize the scattering effect due to the roughness of the SAF structures [as calculated in S3†]. Experiments of such improvements are in progress.

Acknowledgements

This work was financially supported by the Danish Innovationsfonden – the SMARTDETECT project grant no. 118-2012-3 and the Forskningsrådet Teknologi og Produktion (FTP), Sagsnr. 09066487.

Notes and references

1 J. Chan, S. Fore, S. Wachsmann-Hogiu and T. Huser, *Laser Photonics Rev.*, 2008, **2**, 325–349.
2 A. Sandhu, *Nat. Nanotechnol.*, 2007, **2**, 746–748.
3 S. M. Borisov and O. S. Wolfbeis, *Chem. Rev.*, 2008, **108**, 423–461.
4 M. Moskovits, *Rev. Mod. Phys.*, 1985, **57**, 783–826.
5 E. Fort and S. Grésillon, *J. Phys. D: Appl. Phys.*, 2008, **41**, 013001.
6 S.-H. Guo, S.-J. Tsai, H.-C. Kan, D.-H. Tsai, M. R. Zachariah and R. J. Phaneuf, *Adv. Mater.*, 2008, **20**, 1424–1428.
7 S. W. Hell and J. Wichmann, *Opt. Lett.*, 1994, **19**, 780–782.
8 S. W. Hell and M. Kroug, *Appl. Phys. B: Lasers Opt.*, 1995, **60**, 495–497.
9 E. Betzig, *Opt. Lett.*, 1995, **20**, 237–239.
10 E. Betzig, G. H. Patterson, R. Sougrat, O. W. Lindwasser, S. Olenych, J. S. Bonifacino, M. W. Davidson, J. Lippincott-Schwartz and H. F. Hess, *Science*, 2006, **313**, 1642–1645.
11 R. M. Dickson, A. B. Cubitt, R. Y. Tsien and W. E. Moerner, *Nature*, 1997, **388**, 355–358.
12 J. Enderlein, T. Ruckstuhl and S. Seeger, *Appl. Opt.*, 1999, **38**, 724–732.
13 T. Ruckstuhl, J. Enderlein, S. Jung and S. Seeger, *Anal. Chem.*, 2000, **72**, 2117–2123.
14 T. Ruckstuhl, M. Rankl and S. Seeger, *Biosens. Bioelectron.*, 2003, **18**, 1193–1199.
15 T. Ruckstuhl, C. Winterflood and S. Seeger, *Anal. Chem.*, 2011, **83**, 2345–2350.
16 T. Ruckstuhl and D. Verdes, *Opt. Express*, 2004, **12**, 2783–2784.
17 T. Barroca, K. Balaa, J. Delahaye, S. Lévêque-Fort and E. Fort, *Opt. Lett.*, 2011, **36**, 3051–3053.
18 T. Barroca, K. Balaa, S. Lévêque-Fort and E. Fort, *Phys. Rev. Lett.*, 2012, **108**, 218101.
19 D. Kurzbuch, M. Somers and C. McDonagh, *Opt. Express*, 2013, **21**, 22070–22075.
20 C. M. Winterflood, T. Ruckstuhl, D. Verdes and S. Seeger, *Phys. Rev. Lett.*, 2010, **105**, 108103.
21 D. Hill, B. McDonnell, S. Hearty, L. Basabe-Desmonts, R. Blue, M. Trnavsky, C. McAtamney, R. O'Kennedy and B. D. MacCraith, *Biomed. Microdevices*, 2011, **13**, 759–767.
22 X. Li, Y. Ding, J. Shao, H. Tian and H. Liu, *Adv. Mater.*, 2012, **24**, OP165–OP169.
23 Y. Sun, I. Perch-Nielsen, Z. Wang, D. Bang and A. Wolff, in *Micro Total Analysis Systems 2012*, 2012, pp. 1315–1317.
24 Y. Sun, I. Perch-Nielsen, M. Dufva, D. Sabourin, D. D. Bang, J. Høgberg and A. Wolff, *Anal. Bioanal. Chem.*, 2012, **402**, 741–748.
25 E. Berthier, E. W. K. Young and D. Beebe, *Lab Chip*, 2012, **12**, 1224–1237.
26 C. A. Schneider, W. S. Rasband and K. W. Eliceiri, *Nat. Methods*, 2012, **9**, 671–675.